IOSR Journal of Applied Chemistry (IOSR-JAC)
e-ISSN: 2278-5736.Volume 10, Issue 9 Ver. I (September. 2017), PP 21-30
www.iosrjournals.org

NMR, IR and Raman Studies of Diamagnetic Macrocyclic Complexes of 1st Transition Series Metal Ions Exhibiting MLCT Phenomenon: A DFT Application. Part: V. *Tris* (2,2′-bipyridine and 1,10-phenanthroline) Complexes

M. L. Sehgal[1,]* Amit Aggarwal[2,]* Sunaina Singh[2]
[1]*Former Head, Department of Chemistry, D. A. V. College, Jalandhar-144008, Punjab, India.*
[2]*Department of Natural Sciences, LaGuardia Community College, 31-10 Thomson Avenue, Long Island City, New York, 11101, USA*
Corresponding Author:M. L. Sehgal at manoharsehgal@hotmail.com *and*
Amit Aggarwal at aaggarwal@lagcc.cuny.edu

***Abstract**: NMR, IR and Raman spectroscopic studies were used to probe the presence of MLCT phenomenon in four macrocyclic diamagnetic hexa-coordinate complexes: $[L_3Fe]^{2+}$ and $[L_3Co]^{3+}$, where (L= 2,2′-bipyridine and 1,10-phenanthroline) by DFT implemented in ADF.2012.01 After pre-optimization of complexes, the NMR parameters: Chemical Shifts of constituents (δM^{n+}, $\delta^{14}N$, $\delta^{13}C$, and $\delta^{1}H$), their total NMR shielding tensors (σM^{n+}, $\sigma^{14}N$, $\sigma^{13}C$, and $\sigma^{1}H$) containing 2 diamagnetic and 4 paramagnetic contributions, k and j were obtained by using the "NMR Program" with Single Point, LDA or GGA, Default, None, Collinear, Nosym using TZP or TZ2P Basis sets leaving Unrestricted command blank. IR and Raman frequencies of normal modes of Fundamental vibration bands of complexes were obtained by using Frequencies and Raman full key points. Values of two NMR parameters (σ, δ) inferred that the 24 Hydrogens were of 4 different types and all the 6 Nitrogens were of the same type in all of the four studied complexes. However in tris(Bipy) complexes, the 30 Carbons belonged to 5 different types while the 36 Carbons showed 6 different types in tris(Phen) complexes. NMR parameter (H^{Spin}) for all of the four complexes was calculated. The presence of MLCT phenomenon in these complexes was confirmed by a large increase in $\sigma^{14}N$ values for coordinated ligands in these complexes relative to the uncoordinated ligands. The 177 and 195 vibration bands of the two types of complexes respectively were classified into vibration symmetries, IR and Raman activities. Some thermal parameters such as zero point energy, entropy, internal energy and constant volume capacity of the complexes were also calculated and reported here.*

***Keywords**: Chemical Shift, Total NMR Shielding Tensor, Spin-Spin Coupling Constant, Fermi-contact, Effective Spin Hamiltonian*

Date of Submission: 14-08-2017 Date of acceptance: 08-09-2017

I. Introduction

Transition metal complexes have attracted much attention of the current research because of their potential applications in a wide variety of areas including catalysis(*1, 2*), components for water splitting reaction (*3, 4*), energy storage devices(*5*), sensors (*6*) and biologically important materials (*7-11*). A variety of transition metal complexes have been developed so far in which the metal ion binds with the bidentate ligands such as bipyridine(Bipy) and phenthroline (Phen), following the first article published by Fukuda and Sone (*12*).

Investigations of Metal to Ligand Charge Transfer (MLCT) complexes have a rich history (*13-16*), because of their rich optoelectronic and magnetic properties. Transition metal complexes of Ist transition metal series have attracted much attention of the researchers due to a strong desire to synthesize stable photosensitizers using environmentally sustainable materials, replacing more commonly used precious metals such as ruthenium(*17, 18*).

We have recently reported (*19-22*), the use of Computational Chemistry to prove the presence of MLCT phenomenon in macro cyclic 2,2′-bipyridine and 1,10-phenanthroline paramagnetic complexes of 1st transition series metal ions by applying the NMR rather than the commonly used vibration and the electronic spectral techniques.

Here we present the Density Functional Theory (DFT) implemented in ADF 2012.01 to study MLCT phenomenon in four diamagnetic complexes of the two ligands 2,2′-bipyridine and 1,10-phenanthroline where each of these two ligands bind with both Fe(II) and Co(III) metal ions and both having $3d^6$ (t_{2g}^{6}) outermost electronic configuration. The enantioselective interaction of 1,10-phenanthroline complexes of these two metal ions was used as a structural probe and mediators of DNA cleavage reactions (*24-27*). Only a few most relevant papers of these metal ions using DFT would find here a mention here for these tris(bipy) and tris(phen) complexes as follows:

Latevi Max Lawson Daku studied Spin- state crossover phenomenon in low spin $[Fe(bipy)_3]^{2+}$ (*28*) and high spin/low spin energy difference (*29*) while M. Buhl and F.T. Mauschick studied thermal and solvent effects on ^{57}Fe NMR Chemical Shifts (*30, 31*). M. Irwin et al studied the electronic properties of Fe(II) (*23*) bipyridyl radical anion (*32*), Morigakii, Milton. K. et al studied electronic propertied of mixed octahedral 1,10-phenanthroline and 2, 2′-bipyridine complexes of Fe(II) (*23*). Chiniforoshan, H at al (*33*) studied the interaction of Pyrazinamide drug with Co(III) and Zn(II) (*23*) based on 2, 2'-bipyridine and 1, 10-phenanthroline ligands.

Two reasons motivated us to take up this study of four macrocyclic hexa coordinated diamagnetic complexes: $[L_3Fe]^{2+}$, and $L_3Co]^{3+}$ (where L= 2,2′-bipyridine and 1,10-phenanthroline) with D_3 point group as follows:

(a) Like our previously studied 22 paramagnetic complexes (*19-22*), the MLCT character in these four stereo chemically similar diamagnetic complexes was also, never, studied either experimentally or by any computational methods using NMR technique before because accurate computations of their NMR parameters were reported only recently (*34*).

(b) Spatial equivalence among constituents of complexes needed confirmation.

II. Methodology

Different key words were used in ADF software to obtain a number of the IR, Raman and NMR parameters. The mutual relations of NMR parameters given by J. Autschbach (*34*) are shown here for simplicity.

2.1 IR and Raman parameters (*35-37*)

ADF was run with LDA or GGA by replacing Single Point by Geometry Optimization with Default by using TZ P and TZ2P basis sets to save the already pre-optimized complex by "Run" under File menu to click "Read New Coordinates". Geometry Optimization was replaced by Frequencies, Raman full and run to obtain frequencies of normal modes of all the Fundamental IR and Raman bands with their IR (dipole strengths and infrared intensities) and Raman (linear depolarization ratios and Raman intensities) parameters .

2.2 NMR Parameters (*35-37*)

The software was run by filling in certain key words like Single Point, LDA or GGA, Default, None, Collinear, Nosym using TZP orTZ2P Basis sets. The Unrestricted command was left blank. The NMR Program" was run in two steps.

(i) The Shielding Constants of the constituents (σM, $\sigma^{13}C$, and $\sigma^{17}O$) were obtained by clicking on numbers of the species and printing them along with "Isotropic Shielding Constants" and "Full Shielding Constants". The Chemical Shifts (δM, $\delta^{13}C$, and $\delta^{17}O$) were also obtained from the NMR spectra (23).

(ii) **k** and **j** values of constituents were obtained from the same program by using a new Input File and printing numbers of Perturbing and Responding nuclei. The σ values of constituents contained diamagnetic and paramagnetic contributions. Diamagnetic contribution was made up of two terms: diamagnetic core tensor {a} and diamagnetic valence tensor {b}; while the paramagnetic part contained four terms- paramagnetic (b^) tensor {c}, paramagnetic (u^) tensor {d}, paramagnetic (s^) tensor {e} and paramagnetic gauge tensor {f}. These six terms always contributed to the total value of σ in every diamagnetic complex. The software, also, gave Fermi-contact **(k)** and spin-spin coupling (**j**) values.

(a) σM^{n+}, σ^1H, $\sigma^{13}C$ and $\sigma^{14}N$ were equal to the sum of the values of 2 diamagnetic and 4 paramagnetic terms.

(b) δ and σ of ^{1}H and ^{13}C were related as follows:

$$\delta^1H = 31.7 - \sigma^1H \quad \text{-------------------------------} \; (1)$$

$$\delta^{13}C = 181.1 - \sigma^{13}C \quad \text{--------------------------------} \; (2)$$

(c) δM and $\delta^{14}N$ were numerically equal to σM and $\sigma^{14}N$ with reverse signs as follows:

$$\left.\begin{array}{l} \sigma M = -\delta M \\ \\ \sigma^{17}O = -\delta^{14}N \end{array}\right\} \quad \text{--------------------------------} (3)$$

III. Results

Tables: 1A-B showed thermal parameters of complexes. Tables: 2A-B showed optimization parameters of complexes and $M_I.M$ g_n and M_S values of the metals. Tables: 3A-B showed σ and δ values of M^{n+}, ^{14}N, ^{13}C and ^{1}H in complexes. Tables: 4A-B showed 2 diamagnetic and 4 paramagnetic terms (6 in all) in σ values of M^{n+}, ^{14}N, ^{13}C, ^{1}H of complexes. Tables: 5A-B showed ***k, j*** and H^{Spin} values of M^{n+}, ^{14}N, ^{13}C and ^{1}H of complexes.

Tables: 6A-B showed IR and Raman-Active bands of complexes. Table: 7A-B showed $\sigma^{14}N$ values of uncoordinated 2, 2′-bipyridine and 1,10-phenanthroline and complexes.

Figures (1, 2) gave ADF numbers for each of the two tris(2,2′-bipyridine) and tris(1,10-phenanthroline) metal complexes respectively.

Parameter (**j**) was field-independent and mutual ($\mathbf{j}_{AB} = \mathbf{j}_{BA}$). It was affected both by the nature of solvent and metal−ligand bond distances and usually transmitted through bonding electrons. Its magnitude would fall off rapidly with an increase in number of intervening bonds. It might have positive or negative value as it was positive if energy of A was lower when B had opposite spin as A (αβ or βα) and negative if energy of A was lower when B had same spin as A (αα or ββ).

IV. Discussion

Each one of the two tris(bipy) complexes: $[Bipy_3Fe]^{2+}$and $[Bipy_3Co]^{3+}$ having 61 constituents differed only in metal but possessed the same type of 60 atoms: 6 N, 24 H and 30 C while each of the two tris(Phen) complex: $[Phen_3Fe]^{2+}$ and $[Phen_3Co]^{3+}$ with 67 constituents had a different metal but the same type of 66 atoms : 6 N, 24 H and 36 C.

4.1. Calculation of Effective Spin Hamiltonian (H^{Spin}) of M^{n+} and ^{13}C nuclei

Stereo chemically equivalent perturbing and the responding nuclei possessing same values of **k** and **j** parameters in the 4 diamagnetic complexes. Spin-spin coupling parameter **(j)** was related to another important NMR parameter named Effective Spin Hamiltonian (H^{Spin}). It gave a mathematical expression that determined the energy of an NMR transition in a molecule. It was effective in the sense that its solutions reproduce the nuclear magnetic energy levels in a molecular system without reference to electrons. In a fictitious absence of surrounding electrons, the shielding constants and indirect spin-spin coupling constants would vanish leaving the NMR spectrum to be determined by Nuclear Zeeman Term and direct dipolar coupling. A simple relation (4) to calculate Spin Hamiltonian (H^{Spin}) values of the metal ions and the bonded carbon atoms (Tables: 5 A-B) from their **j** values was given below(*34*):

$$H^{Spin} = 6.023\, j_{AB} \cdot I_A \cdot I_B \cdot 10^{17}\ \text{MHz mol}^{-1} \quad \textbf{(4)}$$

4.2. Spatial Equivalence of N, C, H from NMR parameters of complexes

4.2.1. $[Bipy_3M]^{2+}$ {where M=Fe(II) and Co(III)} Complexes

δM^{n+}, $\delta^{14}N$, $\delta^{13}C$, $\delta^{1}H$, σM^{n+}, $\sigma^{14}N$, $\sigma^{13}C$, and $\sigma^{1}H$ of the 61 species in each complex having 2 diamagnetic and 4 paramagnetic terms in their σ values were reported .All the 6 coordinating N atoms were spatially equivalent with one value of each of $\sigma^{14}N$, $\delta^{14}N$ along with the six contributing terms. Both the complexes contained four types of stereo chemically different H; each type possessing six equivalent protons to show four different series of values $\sigma^{1}H$, $\delta^{1}H$ and the 6 contributing terms. The complexes possessed 5 types of spatially different C atoms; each type having 6 equivalents C as they showed five different series of values of $\sigma^{13}C$ and $\delta^{13}C$ and the 6 contributing terms(Table: 4A).

4.2.2. $[Phen_3M]^{2+}$ {where, M=Fe(II) and Co(III)} Complexes

δM^{n+}, $\delta^{14}N$, $\delta^{13}C$, $\delta^{1}H$, σM^{n+}, $\sigma^{14}N$, $\sigma^{13}C$, and $\sigma^{1}H$ of all the 67 species in each one of the two complexes (Table:4B) having six contributing terms in their σ values were reported. All the six coordinating N atoms were spatially equivalent with one value of each of $\sigma^{14}N$, $\delta^{14}N$ and the 6 contributing terms. All these complexes contained four types of stereo chemically different H; each type possessing six equivalent protons to give four different series of values of $\sigma^{1}H$, $\delta^{1}H$ and the 6 contributing terms. The complexes also contained six types of spatially different C atoms; each type having six equivalents C to give six different series of values of $\sigma^{13}C$ and $\delta^{13}C$ and 6 contributing terms (Tables:4B).

4.3. IR and Raman Studies of Complexes

IR and Raman spectra of the four complexes gave definite vibration symmetry symbols of all the fundamental bands and represented a complex by a Vibration Symmetry Class (*38*). Bands were classified according to their IR and Raman activities (Tables: 6 A-B).Contrary to experimental determination (*39-41*), Raman intensities of the complexes were calculated from their polarizabilities (*42-46*).

4.3.1. $[Bipy_3M]$ {where, M=Fe(II) and Co(III)} Complexes

Their 177 fundamental bands were divided into symmetry symbols: A_1, A_2, E containing 30, 29 and 118 bands respectively with Vibration Symmetry Class: {$30A_1 + 29A_2 + 59E$}. They were divided into their IR {A_2 (29), E (59)}, Raman {A_1 (30), A_2 (29), E (59)}, both IR/Raman {A_2 (29), E (59)} activities and 30 A_1 bands were IR inactive. 29 A_2 Raman active bands might not be observed in the Raman spectra because of their negligible Raman intensity {$10^{-28\text{ to }-30}$} (Table: 6A).

4.3.2. [$Phen_3M$] {where, M=Fe(II) and Co(III)} Complexes

All the normal modes of the195 fundamental bands of both the complexes were found to be singly degenerate having **"A"** symmetry with Vibration Symmetry Class [195 A]. All these bands were both IR and Raman active (Table: 6B).

4.4. MLCT Phenomenon from NMR and IR studies

MLCT would result from the shift of electron charge density from molecular orbitals lie mainly metal in character to those with predominantly of ligand character to cause an increase the electron density on the ligand. As σ of any nucleus was directly related to its electron density, any change in its σ value should serve as an indicator to the change in electron density on it. Unlike the paramagnetic complexes (*19-22*) where all the $\sigma^{14}N$, $\sigma^{13}C$, and $\sigma^{1}H$ values were observed to be higher and the $\delta^{14}N$, $\delta^{13}C$, and $\delta^{1}H$ values were found to be lower than their corresponding σ and δ values in the uncoordinated ligands (*19*, *20*), here the σ and δ values of the four diamagnetic complexes showed a slightly different behavior. The $\sigma^{14}N$ and $\delta^{14}N$ values of the N-coordinating sites of these four tris complexes showed changes in the right direction with the $\sigma^{14}N$ values showing an increase (Tables: 7A-B) and $\delta^{14}N$ values exhibiting a decrease to indicate the presence of MLCT phenomenon in these complexes which showed appreciable increase in $\sigma^{14}N$ values to confirm the shift of charge density from the molecular orbitals mainly metal in character to those having predominantly ligands character and, thereby, cause an increase in the electron density on the ligands despite their $\sigma^{13}C$, $\sigma^{1}H$, $\delta^{13}C$, and $\delta^{1}H$, values were found to be comparable to those of the uncoordinated ligands. It was due to the fact that both these metal ions possessing stable filled t_{2g}^{6} set of d orbitals with three sets of paired electrons {Fe(II) and Co(III) =$3d^6$} would be reluctant to transfer their electron cloud to poorly electronegative carbon and hydrogen.

V. Conclusions

(i) NMR technique supported the presence of MLCT phenomenon in the four diamagnetic complexes; analogous to those of our previous studies for 22 paramagnetic complexes as all of them possessed higher $\sigma^{14}N$ values relative to those of the uncoordinated ligand which confirmed an increase in electron density on their ligands i.e. electron cloud gets transferred from the metal into ligand orbitals in both the ligands as per MLCT definition.

(ii) We could, also, justify that these four tris complexes having D_3 symmetry point group possessed similar stereochemistry as all the 60 and 66 constituents in the tris(Bipy) and tris(Phen) complexes respectively were found to occupy the same relative positions around each one of the central metal ion.

Table: 1A. Thermal Parameters of $[Bipy_3M]^{n+}$

$[M]^{n+}$	Zero Point Energy (e V)	Thermal Parameters											
		Entropy (cal mol^{-1} K^{-1})				Internal Energy (Kcal mol^{-1})				Constant Volume Capacity (Kcal mol^{-1} K^{-1})			
		Tran	Rot.	Vib.	Total	Trans.	Rot.	Vib.	Total	Trans	Rot.	Vib.	Total
Fe(II)	12.528	44.63	32.7	69.8	147.14	0.889	0.889	301.7	303.4	2.981	2.981	101.0	107.0
Co(III)	12.551	-do-	-do-	69.3	146.63	-do-	-do-	302.2	303.9	-do-	-do-	100.7	106.7

Table: 1B. Thermal Parameters of $[Phen_3M]^{n+}$

$[M]^{n+}$	Zero Point Energy (e V)	Thermal Parameters											
		Entropy (cal mol^{-1} K^{-1})				Internal Energy (Kcal mol^{-1})				Constant Volume Capacity (Kcal mol^{-1} K^{-1})			
		Tran	Rot.	Vib.	Total	Trans.	Rot.	Vib.	Total	Trans	Rot.	Vib.	Total
Fe(II)	12.528	44.63	32.7	69.8	147.14	0.889	0.889	301.7	303.4	2.981	2.981	101.0	107.0
Co(III)	12.551	-do-	-do-	69.3	146.63	-do-	-do-	302.2	303.9	-do-	-do-	100.7	106.7

Table: 2A. Optimization Parameters ($kJmol^{-1}$), [Mg_n], {M_I} & (M_S) of $[Bipy_3M]^{n+}$

$[M]^{n+}$ (D_3)	[Mg_n], {M_I} (S)	Total bonding energy**	Total Energy : Xc* LDA(Exchange; Correlation)	Nucleus
Fe(II)	[0.181246], {0.5} (0)	-38930.09	-622234.68 -577474.62, -44760.07	^{57}Fe
Co(III)	[1.3220], {3.5},(0)	-37678.63	-631694.02 -586640.77, -45053.25	^{59}Co

Table: 2B. Optimization parameters ($kJmole^{-1}$) of $[Phen_3M]^{n+}$ Complexes

$[M]^{n+}$ (D_3)	[Mg_n] {M_I} (S)	Total bonding energy**	Total Energy : Xc* LDA(Exchange; Correlation)	Nucleus
Fe(II)	[0.181246] {0.5},(0.0)	-45891.30	-696674.17 -646056.22 , -50617.95	^{57}Fe
Co(III)	[1.3220] {3.5}, (0.0)	-44653.93	-706133.68 -655222.52 , -50911.15	^{59}Co

*****Xc is made up of LDA and GGA components; here all have zero GGA
**Bonding energy is computed as an energy difference between molecule and fragments.

Table: 3A. δ and σ values of M^{n+}, N, C, H^a in Diamagnetic $[Bipy_3M]^{n+}$ Complexes [a]

M^{n+} Fig.1	$\delta M^{n+[3]}$ σM^{n+}	$^b\delta N^{[3]}$ $\sigma^{14}N$	$^d\delta H^{[1]}$ σ^1H	$^d\delta H^{[1]}$ σ^1H	$^d\delta H^{[1]}$ σ^1H	$^d\delta H^{[1]}$ σ^1H	$^c\delta C^{[2]}$ $\sigma^{13}C$	$^c\delta C^{[2]}$ $\sigma^{13}C$	$^c\delta C^{[2]}$ $\sigma^{13}C$	$^c\delta C^{[2]}$ $\sigma^{13}C$	$^c\delta C^{[2]}$ $\sigma^{13}C$
	1	7,17,27, 37,47,57	8, 18,28, 38,48,48	9, 19, 29, 39,49,59	10,20,30 40,50,60	11,21,31 41 ,51,61	3, 13, 23, 33,43,53	4, 14, 24, 34,44,54	5,15,25 35,45,55	6,16,26 36 ,46,56	2,12,22 32,42,52
Fe(II)	9402.79 -9402.79	18.29 -18.29	8.07 23.63	7.59 24.11	6.89 24.81	3.71 27.99	118.53 62.57	116.53 64.57	102.94 78.16	134.96 46.14	165.59 15.51
Co(III)	8976.90 -8976.90	-27.74 27.74	8.76 22.94	8.33 23.37	7.52 24.28	2.72 28.98	125.09 56.01	124.01 57.09	107.10 74.00	129.64 51.46	161.88 19.22

Table: 3B. σM^{n+}, σN, σH and δH in Diamagnetic $[Phen_3M]^{n+}$ Complexes [a]

M^{n+}	$\delta M^{n+[3]}$ σM^{n+}	$^b\delta N^{[3]}$ σN	$\delta H^{[1]}$ σH	$\delta H^{[1]}$ σH	$\delta H^{[1]}$ σH	$\delta H^{[1]}$ σH	$\delta C^{[2]}$ σC	$\delta C^{[2]}$ σC	$\delta C^{[2]}$ σC	$\delta C^{[2]}$ σC	$\delta C^{[2]}$ σC	$\delta C^{[2]}$ σC
Fig.2	1	7,17,29, 39,51,61	9,19,31, 41,53,63	10, 2,23, 44,45,66	11,21,33, 43, 55,65	20,32,42, 54,64,67	4,14,26, 36,48,58	5,15,25, 37,49,59	6,16,28, 38,50,60	8,18,30, 40,52,62	3,13,25, 35,47,57	2,12,24, 36,46,56
Fe(II)	10129.7 -10129.7	12.75 -12.75	8.15 23.55	8.27 23.43	6.94 24.76	7.47 24.23	115.0 66.10	110.9 70.20	-131.5 49.61	117.0 64.10	115.94 65.16	126.6 54.47
Co(III)	10774.9 -10774.9	-29.15 29.15	8.85 22.85	8.77 22.93	6.89 24.81	8.01 23.69	122.35 58.75	115.55 65.55	127.92 53.18	116.7 61.40	118.24 62.86	125.54 55.56

[a]ADF Numbers in parentheses[Fig.2]; [b]standard zero; [c]standard 181.1; [d]standard 31.7; Apply Relations [1, 2, 3]

Table: 4A. Sum of Diamagnetic and Paramagnetic contributions in σ of M^{n+}, N, C, and H of $[Bipy_3M]^{n+}$ Complexes [a]

M^{n+} (Fig.1)	σM^{n+} 1		$\sigma^{14}N$ of each of six N 7,17, 27, 37,47,57		σ^1H of 4 types of H each with six H 8, 18, 28, 38,48,48(9,19,29,39,49,49) [10,20,30,40,50,60] {11,21,31,41,51,61}		$\sigma^{13}C$ of 5 types of C each with six C 3, 13, 23, 33,43,53(4,14, 24, 34,44,54) [5,15,25,35,45,55] {6,16,26,36,46,56} {2,12,22,32,42,52}	
	Dia.	Para.	Dia.	Para.	Dia.	Para	Dia.	Para
Fe(II)	2043.3	- 11446.1	321.59	-339.9	27.158 (28.567) [29.905] {32.881}	-3.524 (-4.456) [-5.095] {-4.889}	255.1 (256.8) [259.6] {259.1} {{253.1}}	-192.5 (-192.2) [-181.4] {212.9} {{-237.6}}
Co(III)	2158.0	- 11134.9	321.82	-294.1	26.586 (27.883) [29.314] {32.815}	-3.647 (-4.517) [-5.034] {-3.831}	255.0 (256.8) [259.6] {259.7} {{253.3}}	-199.0 (-199.7) [-185.6] {-208.3} {{-234.1}}

Table: 4B. Sum of Diamagnetic and Paramagnetic, terms [a] in σ values of M^{n+}, N, H, and C of $[Phen_3M]^{n+}$ Complexes [a]

M^{n+} (Fig.2)	σM^{n+} 1		σ^{14}N of each of four N 7,17, 29, 39,51,61		σ^{1}H of four types of H 9,19,31,41,53,63(10, 22,23,44,45,66) [11,21,33,43,45,65] {20,32,42,54,64,67		σ^{13}C of six types of C 4,14,26,36,48,58(5,15,25,37,49,59) [6,16,28, 38,50,60] {8,18,30,40,52,62} {3,13, ,25,35, 47,57} [2,12,24,36,46,56]	
	Dia.	Para.	Dia.	Para.	Dia.	Para.	Dia.	Para.
Fe(II)	2037.9	-12167.6	322.61	-335.4	28.552 (28.602) [29.003] {28.874}	-5.00 (-5.176) [-4.242] {-4.643}	255.7 (256.6) [256.4] {255.1} {{253.3}} [[253.9]]	-189.1 (-186.4) [-206.8] {-191.0} {{-188.1}} [[-199.5]]
Co(III)	2152.1	-12927.1	322.72	-293.6	27.973 (28.086) [28.832] {28.298}	-5.119 (-5.154) [-4.018] {-4.613}	255.9 (256.5) [257.0] {255.1} {{253.5}} [[254.2]]	-197.1 (-191.0) [-203.8] {-193.7} {{-190.6}} [[-198.7]]

[a]ADF Numbers. **Dia**. [Diamagnetic core & valence tensors] **Para.** [Paramagnetic b^, u^, s^ & gauge tensors]

Table: 5A. k, j and H^{spin} values of M^{n+}, N, C and H in Diamagnetic $[Bipy_3M]^{n+}$ complexes (Fig.1)

Perturbing species[a]	Responding species[a]	k[c] and j[d] values	H^{spin} (10^{17} MHz mol^{-1})[b]
	$[Bipy_3Fe]^{2+}$		
Fe(II)(1)	N(7,17,27,3 7,47,57)	160.83,4.51	13.582
N(7,17,27,33 7,47,57)	Fe(II)(1)	--do--	-do-
Fe(II)(1)	Four types of H atoms: (8,18,28,38,48.58) (9,19,29,39,49,59) (10,20,30,40,50,60) (11,21,31,41,51,61)	------- -0.072, -0.028 0.217, 0.084 0.282, 0.109 1.649, 0.640	----- -0.045 0.128 0.166 0.964
Same four types of H atoms	Fe(II)(1)	--do--	-do-
Fe(II)(1)	Five types of C atoms: (2,12,22,32,42,52) (3, 13, 23, 33,43,53) (4, 14, 24, 34,44,54) (5,15,25,35,45,55) (6,16,26,36 ,46,56)	---------- -0.158 , -0.015 2.577, 0.251 -0.447 , -0.044 6.615 , 0.645 7.144 , 0.697	-------- -0.023 0.378 -0.066 0.971 1.050
Same five types of C atoms	Fe(II)(1)	-do-	-do-
	$[Bipy_3Co]^{3+}$		
Co(III)(1)	N(7,17,27,33 7,47,57)	330.20, 67.70	1427.150
N(7,17,27,33 7,47,57)	Co(III)(1)	-do-	-do-
Co(III)(1)	Four types of H atoms: (8,18,28,38,48.58) (9,19,29,39,49,59) (10,20,30,40,50,60) (11,21,31,41,51,61)	---------- -0.145,-0.400 -0.485,1.390 0.475,1.350 0.590,1.670	--------- -4.216 14.651 14.229 17.602
Same four types of H atoms	Co(III) (1)	-do-	-do-
Co(III)(1)	Five types of C atoms: (2,12,22,32,42,52) (3, 13, 23, 33,43,53) (4, 14, 24, 34,44,54) (5,15,25,35,45,55) (6,16,26,36 ,46,56)	---------- -19.082.-13.612 5.135 , 3.663 2.500 , 1.783 6.376 , 4.548 10.841,7.734	--------- -143.474 38.609 18.793 47.937 81.518
Same five types of C atoms	Co(III) (1)	-do-	-do-

Table: 5B. k, j and H^{spin} values of M^{n+}, N, C and H in Diamagnetic $[Phen_3M]^{n+}$ complexes (Fig.2)

Perturbing Species [a]	Responding Species [a]	k^c and j^d values	H^{spin} (10^{17} MHz mol^{-1})[b]
	$[Phen_3Fe]^{2+}$		
Fe(II)(1)	N(7,17,29, 39, 51,61)	160.835,4.510 150.315 4.215	13.582
N(7,17,29, 39, 51,61)	Fe(II)(1)	--do--	-do-
Fe(II)(1)	Four types of H atoms: (9,19,31,41,53.63) (10,22,23,44,45,66) (11,21,33,43,55,65) (20,32,42,54,64,67)	---------- 0.228 , 0.088 0.095 , 0.037 0.958 ,0.372 0.364 ,0.141	------ -0.542 0.075 -0.75 0.437
Same four types of H atoms	Fe(II)(1)	--do--	-do-
Fe(II)(1)	Six types of C atoms: (2,12,24,36,46,56) (3,13,25,35,47,57) (4,14,26,36,48,58) (5,15,25,37,49,59) (6,16,28,38,50,60) (8,18,30,40,52,62)	------------ 6.659 , 0.650 3.703 , 0.361 -0.323 , -0.031 4.823 ,0.471 6.129 , 0.598 0.727 , 0.071	------- 0.979 0.544 -0.047 0.709 0 .900 0.107
Same Six types of C atoms	Fe(II)(1)		
	$[Phen_3Co]^{3+}$		
Co(III)(1)	N(7,17,29, 39, 51,61)	156.590, 32.106	677.106
N(7,17,29, 39, 51,61)	Co(III)(1)	--do--	-do-
Co(III)(1)	Four types of H atoms: (9,19,31,41,53.63) (10,22,23,44,45,66) (11,21,33,43,55,65) (20,32,42,54,64,67)	----------- 0.095,0.270 0.085,0.240 0.968, 2.745 0.413,1.171	------ 2.846 2.530 28.986 12.279
Same four types of H atoms	Co(III)(1)	--do--	-do-
Co(III)(1)	Six types of C atoms: (2,12,24,36,46,56) (3,13,25,35,47,57) (4,14,26,36,48,58) (5,15,25,37,49,59) (6,16,28,38,50,60) (8,18,30,40,52,62)	------------ 7.512 , 5.359 3.696 , 2.637 -0.436 , -0.311 4.757 , 3.393 6.527 , 4.656 0.740, 0.528	------- 56.485 27.795 -3.278 35.763 49.075 5.565
Same Six types of C atoms	Co(III)(1)		

[a]ADF Numbers in parentheses [Fig: 2]. [b]Apply Relation (6). [c][10^{19} kg $m^{-2}s^{-2}$ A^{-2}]. [d]ppm

Table: 6A. Designation of IR/Raman Bands and Their Vibration Symmetry Classes

Complex [D_3] (Fig.1)	Vibration Symmetries of bands*	IR active bands	Raman active bands	Both IR and Raman active bands	IR inactive bands	Raman inactive bands	Raman bands not[a] observed	Vibration symmetry Class
$[Bipy_3Fe]^{2+}$	A_1(30)	A_2(29)	A_1(30)	A_2(29)	A_1(30)	----	A_2[a] (29)	[$30A_1$+$29A_2$+59E]
$Bipy_3Co]^{3+}$	A_2(29)	E(59)	A_2(29)[a]	E(59)	----	----	---	
	E(59)	---	E(59)	----	----	----	----	
	A_2(29)	E(59)	A_2(29)[a]	E(59)	----	----	---	
	E(59)	----	E(59)	----	----	---	---	

Table: 6B. Designation of IR/Raman Bands and Their Vibration Symmetry Classes

Complex [D_3] (Fig.2)	Vibration Symmetries of bands*	IR Active bands	Raman Active bands	Both IR and Raman active bands	IR inactive bands	Raman inactive bands	Raman not[a] observed	Vibration Symmetry Class
$[Phen_3Fe]^{2+}$, $[Phen_3Co]^{3+}$	A(195)	A(195)	A(195)	A(195)	---	----	---	**[195A]**

*Numbers in parentheses indicate bands. [a]Raman active; but intensity being $10^{-29\ to\ -30}$; not observed.

Table: 7A. σN values of 2, 2′-Bipyridine ligand and its complexes

	2, 2′-Bipyridine	**$[Bipy_3Fe]^{2+}$**	**$[Bipy_3Co]^{3+}$**
σ N	(6) -124.7; (16) -132.4	-18.29	27.74

Table: 7B. σN values of 1,10-Phenanthroline ligand and its complexes

	1,10-Phenanthroline	**$[Phen_3Fe]^{2+}$**	**$[Phen_3Co]^{3+}$**
σ N	-138.4	-12.75	29.15

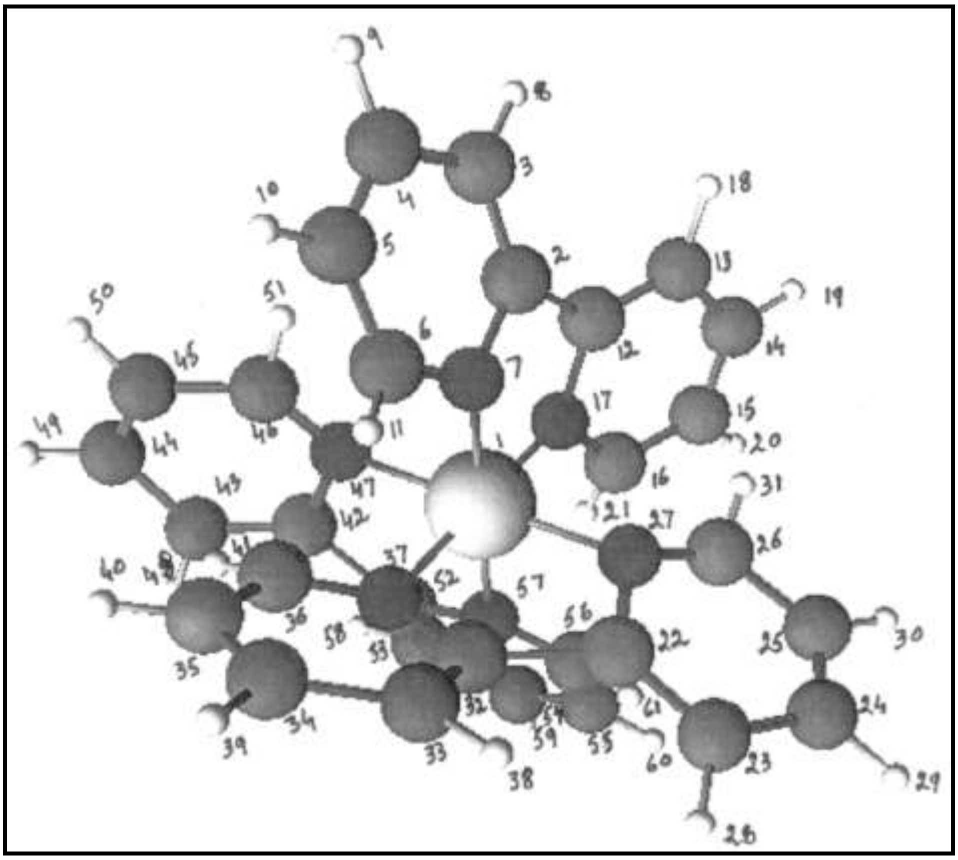

Fig.1 Fe(II) and Co(III) are shown as number 1 position atom.

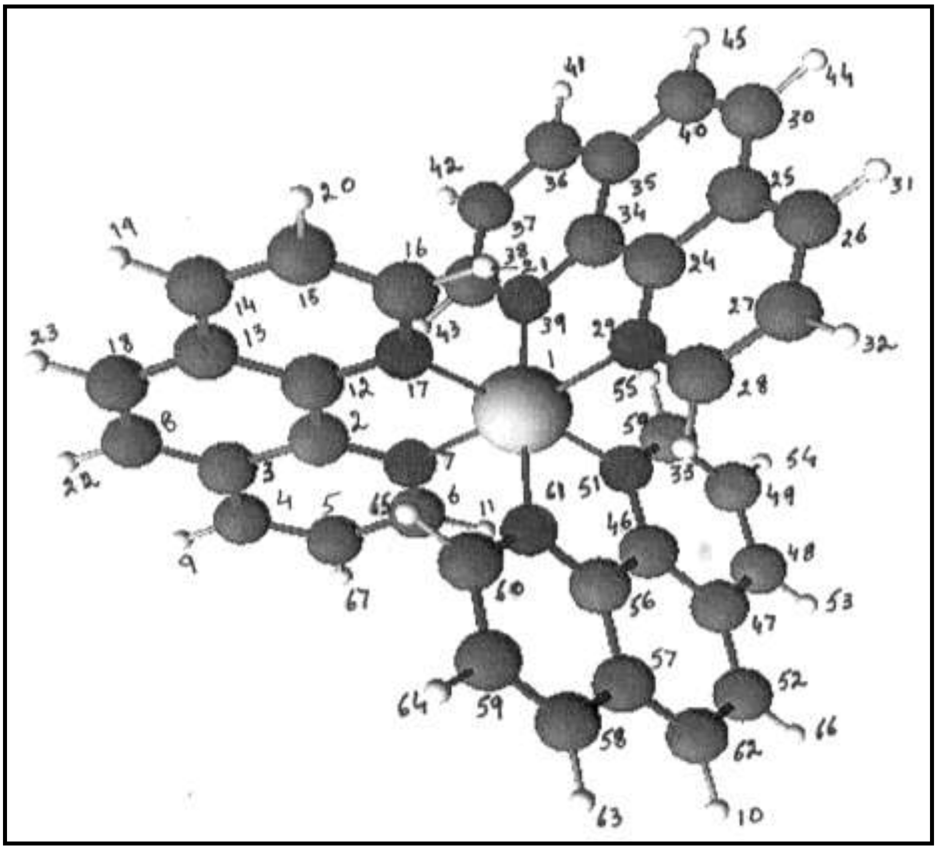

Fig.2: Fe(II) and Co(III) are shown as number 1 atom.

References

[1] Soriego, R., Farias, L., and Moya, S. A. (1997) Complexes with heterocyclic nitrogen ligands—IV: complexes of ruthenium(II) and applications in catalysis, Polyhedron 16, 3847-3850.

[2] Gupta, K. C., and Sutar, A. K. (2008) Catalytic activities of Schiff base transition metal complexes, Coord. Chem. Rev. 252, 1420-1450.

[3] Pérez-Arredondo, M. d. l. L., González-Ponce, M. d. R., Ana Zanor, G., Ramirez Vazquez, J. A., and Segoviano-Garfias, J. J. N. (2015) Complex formation equilibria of 2,2′-bipyridyl and 1,10-phenanthroline with manganese(II) in methanol, Kar. Int. J. Mod. Sci. 1, 178-186.

[4] Liu, X., and Wang, F. (2012) Transition metal complexes that catalyze oxygen formation from water: 1979–2010, Coord. Chem. Rev. 256, 1115-1136.

[5] Zheng, Q., Niu, Z., Ye, J., Zhang, S., Zhang, L., Li, L., Zhao, Y., and Zhang, X. (2017) High Voltage, Transition Metal Complex Enables Efficient Electrochemical Energy Storage in a Li-Ion Battery Full Cell, Adv. Funct. Mater. 27, 1604299.

[6] Harvey, E. C., Feringa, B. L., Vos, J. G., Browne, W. R., and Pryce, M. T. (2015) Transition metal functionalized photo- and redox-switchable diarylethene based molecular switches, Coord. Chem. Rev. 282–283, 77-86.

[7] Mathan Kumar, S., Dhahagani, K., Rajesh, J., Nehru, K., Annaraj, J., Chakkaravarthi, G., and Rajagopal, G. (2013) Synthesis, characterization, structural analysis and DNA binding studies of nickel(II)–triphenylphosphine complex of ONS donor ligand – Multisubstituted thiosemicarbazone as highly selective sensor for fluoride ion, Polyhedron 59, 58-68.

[8] Prashanthi, Y., Kiranmai, K., Ira, kumar K, S., Chityala, V. k., and Shivaraj. (2012) Spectroscopic Characterization and Biological Activity of Mixed Ligand Complexes of Ni(II) with 1,10-Phenanthroline and Heterocyclic Schiff Bases, Bioinorg. Chem. Appl. 2012, 1-8.

[9] Kani, I., Atlier, Ö., and Guven, K. (2016) Mn(II) complexes with bipyridine, phenanthroline and benzoic acid: Biological and catalase-like activity, J. Chem. Sci. 128, 523-536.

[10] Ronconi, L., and Sadler, P. J. (2007) Using coordination chemistry to design new medicines, Coord. Chem. Rev. 251, 1633-1648.

[11] Biswas, B., Kole, N., Patra, M., Dutta, S., and Ganguly, M. (2013) Synthesis, structural characterization and biological activity of a trinuclear zinc(II) complex: DNA interaction study and antimicrobial activity, J. Chem. Sci. 125, 1445-1453.

[12] Fukuda, Y., and Sone, K. (1970) Formation and Absorption Spectra of Mixed Copper(II) Chelates Containing Acetylacetone and 2,2′-Bipyridine or 1,10-Phenanthroline, Bull. Chem. Soc. Jpn. 43, 556-558.

[13] Wehry, E. L., and Sundararajan, S. (1972) Intersystem crossing and internal conversion from the lowest charge-transfer singlet excited state of the (2,9-dimethyl-1,10-phenanthroline)copper(I) cation, J. Chem. Soc. Chem. Commun., 1135-1136.

[14] Blaskie, M. W., and McMillin, D. R. (1980) Photostudies of copper(I) systems. 6. Room-temperature emission and quenching studies of bis(2,9-dimethyl-1,10-phenanthroline)copper(I), Inorg. Chem. 19, 3519-3522.

[15] Ashbrook, L. N., and Elliott, C. M. (2013) Dye-Sensitized Solar Cell Studies of a Donor-Appended Bis(2,9-dimethyl-1,10-phenanthroline) Cu(I) Dye Paired with a Cobalt-Based Mediator, J. Phys. Chem. C 117, 3853-3864.

[16] Garakyaraghi, S., Crapps, P. D., McCusker, C. E., and Castellano, F. N. (2016) Cuprous Phenanthroline MLCT Chromophore Featuring Synthetically Tailored Photophysics, Inorg. Chem. 55, 10628-10636.

[17] Indelli, M. T., Bignozzi, C. A., Scandola, F., and Collin, J.-P. (1998) Design of Long-Lived Ru(II) Terpyridine MLCT States. Tricyano Terpyridine Complexes, Inorg. Chem. 37, 6084-6089.

[18] Turro, C., Bossmann, S. H., Leroi, G. E., Barton, J. K., and Turro, N. J. (1994) Ligand-Specific Charge Localization in the MLCT Excited State of $Ru(bpy)_2(dpphen)^{2+}$ Monitored by Time-Resolved Resonance Raman Spectroscopy, Inorg. Chem. 33, 1344-1347.

[19] Sehgal, M. L., and Ahmad, I. (2017 (accepted)) NMR, ESR,NQR and IR studies of paramagnetic macro cyclic complexes of 1^{st} transition series metal ions exhibiting MLCT phenomenon: A Density Functional Theory application:Part:I Bis (2, 2'- bipyridine) complexes, Orient. J. Chem.

[20] Sehgal, M. L., and Ahmad, I. (2017) NMR, ESR,NQR and IR studies of paramagnetic macro cyclic complexes of 1^{st} transition series metal ions exhibiting MLCT phenomenon: A Density Functional Theory application:Part:II Bis (1,10- phenanthroline) complexes, Orient. J. Chem. 33, 1714-1725.

[21] Sehgal, M. L., Aggarwal, A., and Singh, S. (2017) NMR, ESR, NQR and IR Studies of Paramagnetic Macrocyclic Complexes of 1st Transition Series Metal Ions Exhibiting MLCT Phenomenon: A DFT Application. Part: III. Tris(2, 2'-bipyridine) Complexes, IOSR- J. Appl. Chem. 10, 78-84.

[22] Sehgal, M. L., Aggarwal, A., and Singh, S. (2017) NMR, ESR, NQR and IR Studies of Paramagnetic Macrocyclic Complexes of 1st Transition Series Metal Ions Exhibiting MLCT Phenomenon: A DFT Application. Part: IV. Tris(1, 10-phenanthroline) Complexes, IOSR- J. Appl. Chem. 10, 16-22.

[23] MorigakiI, M. K., Silva, E. M. d., Melo, C. V. P. d., Pavan, J. R., Silva, R. C., Biondo, A., Freitas, J. C. C., and Dias, G. H. M. (2009) Synthesis, characterization, DFT and Td-dfT study of the $[Fe(mnt)(L)(t\text{-}BuNC)_2]$ octahedral complex (L = phen, bipy), Química Nova 32, 1812-1817.

[24] Mudasir, Wijaya, K., Tjahjono, D. H., Yoshioka, N., and Inoue, H. (2004) DNA-Binding Properties of Iron(II) Mixed-Ligand Complexes Containing 1,10-Phenanthroline and Dipyrido[3,2-a:2’,3’-c]phenazine, znb 59b, 310-318.

[25] Sreekanth, B., Krishnamurthy, G., Naik, H. S. B., Vishnuvardhan, T. K., Shashikumar, N. D., and Lokesh, M. R. (2011) DNA Binding and Cleavage Studies of Fe(II) and Zn(II) Complexes containing Mixed Ligand of 1,10-phenanthroline and 2-hydroxy-4-methyl-1,8-naphthyridine, J. Chem. Pharm. Res. 3, 407-419.

[26] Sreekanth, B., Krishnamurthy, G., Naik, H. S. B., Vishnuvardhan, T. K., Vinaykumar, B., and Sharath, N. (2011) Synthesis, DNA Binding, and Oxidative Cleavage Studies of Fe(II) and Co(III) Complexes Containing Bioactive Ligands, Nucleosides Nucleotides Nucleic Acids 30, 83-96.

[27] Sreekanth, B., Krishnamurthy, G., Naik, H. S. B., and Vishnuvardhan, T. K. (2012) Cu(II) and Mn(II) Complexes Containing Macroacyclic Ligand: Synthesis, DNA Binding, and Cleavage Studies, Nucleosides Nucleotides Nucleic Acids 31, 1-13.

[28] Latevi Max Lawson, D. (2013) Modeling Transition Metal Complexes in the Framework of the Spin-Crossover Phenomenon: A DFT Perspective, Curr. Inorg. Chem. 3, 242-259.

[29] Lawson Daku, L. M., Vargas, A., Hauser, A., Fouqueau, A., and Casida, M. E. (2005) Assessment of Density Functionals for the High-Spin/Low-Spin Energy Difference in the Low-Spin Iron(II) Tris(2,2′-bipyridine) Complex, ChemPhysChem 6, 1393-1410.

[30] Buhl, M., and Mauschick, F. T. (2002) Thermal and solvent effects on ^{57}Fe NMR chemical shifts, Phys. Chem. Chem. Phys. 4, 5508-5514.

[31] Bühl, M., Mauschick, F. T., Terstegen, F., and Wrackmeyer, B. (2002) Remarkably Large Geometry Dependence of ^{57}Fe NMR Chemical Shifts, Angew. Chem. Int. Ed. 41, 2312-2315.

[32] Irwin, M., Jenkins, R. K., Denning, M. S., Krämer, T., Grandjean, F., Long, G. J., Herchel, R., McGrady, J. E., and Goicoechea, J. M. (2010) Experimental and Computational Study of the Structural and Electronic Properties of FeII(2,2′-bipyridine)(mes)2 and [FeII(2,2′-bipyridine)(mes)2]−, a Complex Containing a 2,2′-Bipyridyl Radical Anion, Inorg. Chem. 49, 6160-6171.

[33] Chiniforoshan, H., Radani, Z. S., Tabrizi, L., Tavakol, H., Sabzalian, M. R., Mohammadnezhad, G., Görls, H., and Plass, W. (2015) Pyrazinamide drug interacting with Co(III) and Zn(II) metal ions based on 2,2′-bipyridine and 1,10-phenanthroline ligands: Synthesis, studies and crystal structure, DFT calculations and antibacterial assays, J. Mol. Struc. 1081, 237-243.

[34] Autschbach, J. (2004) The Calculation of NMR Parameters in Transition Metal Complexes, In Principles and Applications of Density Functional Theory in Inorganic Chemistry I (Kaltsoyanis, N., and McGrady, J. E., Eds.), pp 1-43, Springer Berlin Heidelberg, Berlin, Heidelberg.

[35] Sharma, S., Chander, S., Sehgal, M. L., and Ahmad, I. (2015) ^{13}C and ^{17}O NMR of Mono-Nuclear Carbonyls: A DFT Study, Orient. J. Chem. 31, 1417-1427.

[36] Singh, H., Bhardwaj, A. K., Sehgal, M. L., and Ahmad, I. (2015) Predicting ESR Peaks in Copper (II) Chelates Having Quadrupolar Coordinating Sites by NMR, ESR and NQR Techniques: A DFT Study, Orient. J. Chem. 31, 671-679.

[37] Singh, H., Bhardwaj, A. K., Sehgal, M. L., Javed, M., and Ahmad, I. (2015) Predicting ESR Peaks in Titanium (III), Vanadium (IV) and Copper (II) Complexes of Halo Ligands by NMR, ESR and NQR Techniques: A DFT Study, Orient. J. Chem. 31, 1461-1468.

[38] Nakamoto, K. (1986) Infrared and Raman Spectra of Inorganic and Coordination Compounds, 4th Ed. ed., John Wiley & Sons Inc.

[39] Ryason, P. R. (1962) Raman band intensities in binary liquid solutions, J. Mol. Spectroscopy 8, 164-166.

[40] Schrötter, H. W., and Bernstein, H. J. (1964) Intensity in the Raman effect. IX. Absolute intensities for some gases and vapors, J. Mol. Spectroscopy 12, 1-17.

[41] Long, D. A., Gravenor, R. B., and Milner, D. C. (1963) Intensities in Raman spectra. Part 8.-Intensity measurements in CHCl3 and CDCl3, Trans. Farad. Soc. 59, 46-52.

[42] Gisbergen, S. J. A. v., Snijders, J. G., and Baerends, E. J. (1995) A density functional theory study of frequency- dependent polarizabilities and Van der Waals dispersion coefficients for polyatomic molecules, J. Chem. Phys. 103, 9347-9354.

[43] Gisbergen, S. J. A. v., Osinga, V. P., Gritsenko, O. V., Leeuwen, R. v., Snijders, J. G., and Baerends, E. J. (1996) Improved density functional theory results for frequency-dependent polarizabilities, by the use of an exchange- correlation potential with correct asymptotic behavior, J. Chem. Phys. 105, 3142-3151.

[44] van Gisbergen, S. J. A., Snijders, J. G., and Baerends, E. J. (1996) Application of time-dependent density functional response theory to Raman scattering, Chem. Phys. Lett. 259, 599-604.

[45] Osinga, V. P., Gisbergen, S. J. A. v., Snijders, J. G., and Baerends, E. J. (1997) Density functional results for isotropic and anisotropic multipole polarizabilities and C6, C7, and C8 Van der Waals dispersion coefficients for molecules, J. Chem. Phys. 106, 5091-5101.

[46] van Gisbergen, S. J. A., Kootstra, F., Schipper, P. R. T., Gritsenko, O. V., Snijders, J. G., and Baerends, E. J. (1998) Density-functional-theory response-property calculations with accurate exchange-correlation potentials, Phys. Rev. A 57, 2556-2571.

IOSR Journal of Applied Chemistry (IOSR-JAC) is UGC approved Journal with Sl. No. 4031, Journal no. 44190.

M. L. Sehgal. "NMR, IR and Raman Studies of Diamagnetic Macrocyclic Complexes of 1st Transition Series Metal Ions Exhibiting MLCT Phenomenon: A DFT Application. Part: V.Tris (2,2□-Bipyridine and 1,10-Phenanthroline) Complexes." IOSR Journal of Applied Chemistry (IOSR-JAC), vol. 10, no. 9, 2017, pp. 21–30.